

Tilt adjustment for a portable absolute atomic gravimeter

Hong-Tai Xie(谢宏泰), Bin Chen(陈斌), Jin-Bao Long(龙金宝), Chun Xue(薛春), Luo-Kan Chen(陈泺侃), Shuai Chen(陈帅)

Citation: Chin. Phys. B . 2020, 29(7): 073701 . **doi:** 10.1088/1674-1056/ab90f9
Journal homepage: http://cpb.iphy.ac.cn; http://iopscience.iop.org/cpb

What follows is a list of articles you may be interested in

Calibration of the superconducting gravimeter based on a cold atom absolute gravimeter at NIM

Qiyu Wang(王启宇), Jinyang Feng(冯金扬), Shaokai Wang(王少凯), Wei Zhuang(庄伟), Yang Zhao(赵阳), Lishuang Mou(牟丽爽), Shuqing Wu(吴书清)

Chin. Phys. B . 2018, 27(12): 123701 . **doi:** 10.1088/1674-1056/27/12/123701

Strontium optical lattice clock at the National Time Service Center

Ye-Bing Wang(王叶兵), Mo-Juan Yin(尹默娟), Jie Ren(任洁), Qin-Fang Xu(徐琴芳), Ben-Quan Lu(卢本全), Jian-Xin Han(韩建新), Yang Guo(郭阳), Hong Chang(常宏)

Chin. Phys. B . 2018, 27(2): 023701 . **doi:** 10.1088/1674-1056/27/2/023701

Comparison of the sensitivities for atom interferometers in two different operation methods

Xiao-Chun Duan(段小春), De-Kai Mao(毛德凯), Xiao-Bing Deng(邓小兵), Min-Kang Zhou(周敏康), Cheng-Gang Shao(邵成刚), Zhu Zhu(祝竺), Zhong-Kun Hu(胡忠坤)

Chin. Phys. B . 2018, 27(1): 013701 . **doi:** 10.1088/1674-1056/27/1/013701

Common-mode noise rejection using fringe-locking method in WEP test by simultaneous dual-species atom interferometers

Xiao-Bing Deng(邓小兵), Xiao-Chun Duan(段小春), De-Kai Mao(毛德凯), Min-Kang Zhou(周敏康), Cheng-Gang Shao(邵成刚), Zhong-Kun Hu(胡忠坤)

Chin. Phys. B . 2017, 26(4): 043702 . **doi:** 10.1088/1674-1056/26/4/043702

Investigation of the thermal adaptability for a mobile cold atom gravimeter

Qi-Yu Wang(王启宇), Zhao-Ying Wang(王兆英), Zhi-Jie Fu(付志杰), Qiang Lin(林强)

Chin. Phys. B . 2016, 25(12): 123701 . **doi:** 10.1088/1674-1056/25/12/123701

Tilt adjustment for a portable absolute atomic gravimeter*

Hong-Tai Xie(谢宏泰)[1,2,3], Bin Chen(陈斌)[1,2,3], Jin-Bao Long(龙金宝)[1,2,3], Chun Xue(薛春)[4], Luo-Kan Chen(陈泺侃)[1,2,3], and Shuai Chen(陈帅)[1,2,3,†]

[1] *Hefei National Laboratory for Physical Sciences at the Microscale and Department of Modern Physics, University of Science and Technology of China, Hefei* 230026, *China*

[2] *Shanghai Branch, CAS Center for Excellence in Quantum Information and Quantum Physics, University of Science and Technology of China, Shanghai* 201315, *China*

[3] *Shanghai Research Center for Quantum Sciences, Shanghai* 201315, *China*

[4] *Shanghai Division, QuantumCTek Co., Ltd. Shanghai* 201315, *China*

(Received 19 February 2020; revised manuscript received 30 April 2020; accepted manuscript online 7 May 2020)

For an atomic gravimeter, the measured value of the Earth's gravity acceleration g is the projection of the local gravity on the direction of Raman laser beams. To accurately measure the g, the Raman laser beams should be parallel to the g direction. We analyze the tilt effect of the Raman beams on g measurement and present a general method for the tilt adjustment. The systematic error caused by the tilt angle is evaluated as 0 $(+0, -0.8)$ μGal (1 μGal = 10 nm/s^2) and the drift is also compensated in real time. Our method is especially suitable for the portable atomic gravimeter which focuses on the mobility and field applications.

Keywords: atomic gravimeter, systematic error, tilt adjustment, stability

PACS: 37.25.+k, 03.75.Dg, 06.20.–f **DOI:** 10.1088/1674-1056/ab90f9

1. Introduction

Measurement of the Earth's gravity acceleration g is important for numerous scientific studies and applications, such as the new definition of kilogram,[1] geodesy, geophysics, resources exploration,[2] and autonomous navigation.[3] The best-performing gravimeters at present time include relative gravimeters[4,5] and falling corner cube gravimeters[6–8] based on optical interferometry. With these high performing instruments, researchers can measure g in a very high sensitivity and accuracy (up to μGal level). Cold atomic gravimeters based on matter wave interferometry have been rapidly developed since the 1990s[9–20] and have achieved extremely high sensitivity[21] and stability[22] that had advanced to the high performing falling corner cube gravimeters. The comparison of absolute gravimeters shows that the degree of equivalence and the uncertainty of atomic gravimeters also reach several μGal (1 μGal = 10 nm/s^2)[23] and ready to be used in real applications.

Based on the two-photon Raman transition between two hyperfine levels of the atom ground state, a $\pi/2$–π–$\pi/2$ Raman pulse sequence splits, reflects, and recombines the atomic wave packet for the interferomety.[9] The phase shift due to the gravity is as follows:

$$\Delta\Phi = \boldsymbol{k}_{\text{eff}} \cdot \boldsymbol{g} \cdot T^2, \tag{1}$$

where $\Delta\Phi$ is the phase shift of the interferometer, $\boldsymbol{k}_{\text{eff}}$ is the effective wave vector of the Raman lasers and T is the interogation time between the Raman pulses. From Eq. (1), the measured value of g is the projection of $\boldsymbol{g}$ onto the $\boldsymbol{k}_{\text{eff}}$ direction. The accuracy is partly dependent on the tilt angles of the Raman lasers of the atom interferometer.[11]

Researchers have made considerable efforts to correct the systematic error caused by tilt, such as calibrating the direction of the incident beam with a liquid surface,[24] determining the orientation of the mirror with an electronic bubble level,[11] calibrating the directions of the Raman beams with a beam-splitter and a CCD camera,[25] and adjusting the reflected beam overlap the incident beam with a photo-diode.[26] These methods are suitable for atomic gravimeters in labs or fixed stations, but too complicated for the portable atomic gravimeters. There are also some methods that meet the portable demand. For example, use a corner cube mirror to make the reflected beam overlap the incident beam,[27] but may cause worse wavefront aberrations;[28–30] and adjust the directions of the incident beam and reflected beam for parabola fitting respectively,[31] but the direction of the reflected beam is not independent of incident beam, which induces a cross term and makes the adjustment invalid.

In this paper, we provide a common approach for the tilt adjustment of the Raman laser beams in a portable absolute atomic gravimeter. By applying this approach, the systematic error of our portable atomic gravimeter USTC-AG02 ac-

*Project supported by the National Key R&D Program of China (Grant No. 2016YFA0301601), the National Natural Science Foundation of China (Grant No. 11674301), Anhui Initiative in Quantum Information Technologies, China (Grant No. AHY120000), and Shanghai Municipal Science and Technology Major Project, China (Grant No. 2019SHZDZX01).

†Corresponding author. E-mail: shuai@ustc.edu.cn

© 2020 Chinese Physical Society and IOP Publishing Ltd

cording to the tilt is effectively eliminated, becomes 0 (+0, −0.8) μGal considering the uncertainty. Also, with continuous tilt monitoring, the compensation for the measured g value is applied to enhance the long term accuracy. This approach especially fit for the gravimeter adjustment in the field applications.

2. The atomic gravimeter

The absolute atomic gravimeter USTC-AG02 is based on the Mach–Zehnder type atom interferometer. The schematic diagram of the gravimeter's sensor is shown in Fig. 1(a). The Raman lasers and the vertical cooling laser are combined and injected into the vacuum chamber from the top. They are retro-reflected by a vibration-isolated mirror to form the counter-propagating scheme. The additional four cooling beams were horizontally shine into the vacuum in the magneto-optical trap (MOT) area. In the detection area, the probe lasers are applied to excite the falling atoms to generate the resonant florescence for $F = 2$ and $F = 1$, respectively. For each g-measurement circle, about 10^8 cold ^{87}Rb atoms were captured by the MOT and further cooled down to 5 μK by the polarization-gradient cooling in 100 ms. For initial state preparation, a series of Raman pulses are applied to prepare the atoms in the $|F = 1, m_F = 0\rangle$ initial state, with the vertical temperature of 300 nK and remaining atoms of around 10^6. During the free-falling, the interferometry was realized by the $\pi/2$–π–$\pi/2$ Raman pulse sequence with the interogation time of $T = 90$ ms. Finally, the florescence of the atoms are collected in the detection zone to get the population in both the $|2,0\rangle$ and $|1,0\rangle$ states. The probability in the $F = 2$ state was normalized as[11]

$$P_{|F=2\rangle} = \frac{1}{2}(1 - A\cos\Delta\Phi), \tag{2}$$

where A is the contrast of the interferometry signal and the $\Delta\Phi$ is the phase shift induced by the gravity as shown in Eq. (1).

The Raman beams entered the vacuum chamber through a fiber collimator with a 45° mirror (Fig. 1(b)) and were reflected back by a vibration isolated 0° reflective mirror (Fig. 1(c)). The tilting angle of the downward and upward beams could be precisely tuned by the fine-adjustment screws with electronic actuators. The two biaxial tilt meters that recorded the tilting angles were mounted on the fiber collimator and 0° reflective mirror, respectively. The tilt meter on top recorded the tilting angles α_x and α_y of the downward Raman laser, and the bottom one recorded the tilting angles β_x and β_y of the reflective mirror in x and y directions, respectively. The four angle readings (α_x, α_y, β_x, and β_y) were set to be independently controlled by the four actuators. In order to get rid of the cross-talk during the adjustment, the axes of the actuators and the correspond tilt meter are all aligned parallel to the framework of gravimeter, with the mounting error less than 0.5°.

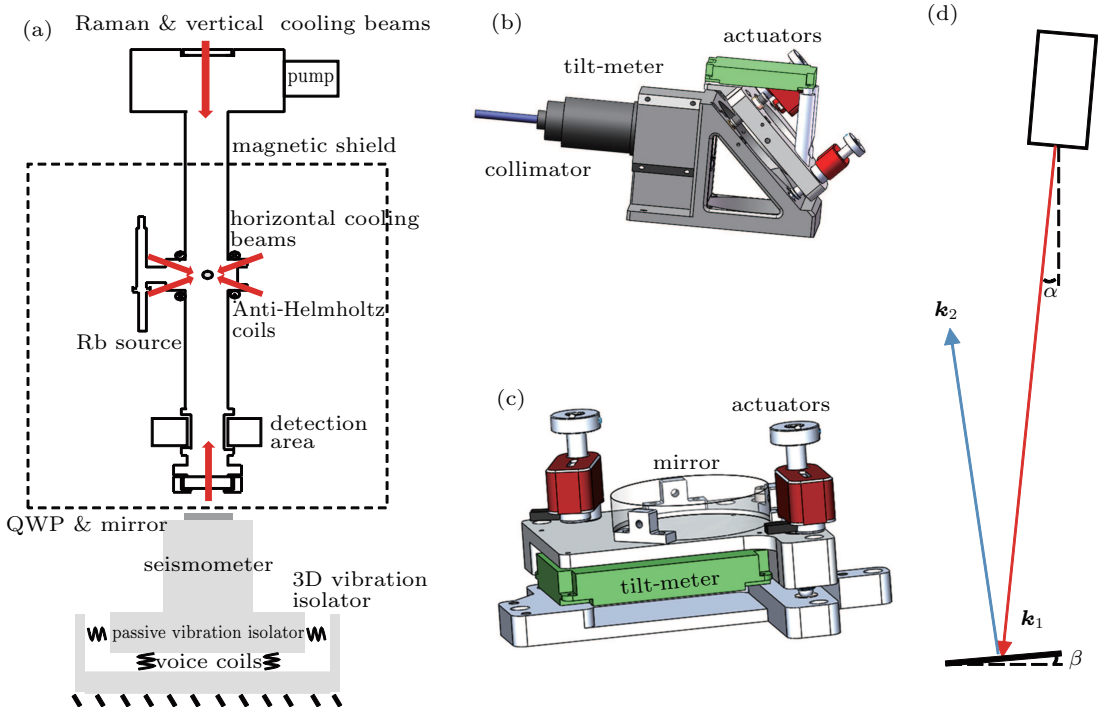


Fig. 1. (a) Schematic diagram of the USTC-AG02 sensor. It includes an atom interferometer, a magnetic shield, and a 3D vibration isolator. (b) Illustration of the Raman beam collimator on top of the vacuum chamber. (c) Illustration of the retro-reflector on the bottom of the vacuum chamber. (d) The Raman beam comprises of two counter-propagation beams, with wave vectors of $\boldsymbol{k}_1$ and $\boldsymbol{k}_2$. Here α is the tilting angle of $\boldsymbol{k}_1$, and β is the tilting angle of the retro-reflection mirror. The angle between $\boldsymbol{k}_2$ and $\boldsymbol{g}$ is $\pi - (2\boldsymbol{\beta} - \boldsymbol{\alpha})$.

3. Method: Tilt adjustment

The direction analysis of the effective wave-vector $\boldsymbol{k}_{\rm eff}$ is shown in Fig. 1(d). Consider about the tilting angle, the phase shift of the gravimeter is given by[25]

$$\begin{aligned}\Delta\Phi &= \boldsymbol{k}_{\rm eff}\cdot\boldsymbol{g}\cdot T^2\\ &= (\boldsymbol{k}_1-\boldsymbol{k}_2)\cdot\boldsymbol{g}\cdot T^2\\ &= (|\boldsymbol{k}_1|\cos\boldsymbol{\alpha}+|\boldsymbol{k}_2|\cos(2\boldsymbol{\beta}-\boldsymbol{\alpha}))|\boldsymbol{g}|T^2. \end{aligned}\tag{3}$$

Because $|\boldsymbol{k}_1|\approx|\boldsymbol{k}_2|\approx|\boldsymbol{k}_{\rm eff}|/2$ and α and β are small angles, we have

$$\Delta\Phi=(1-\alpha^2/2-\beta^2+\boldsymbol{\alpha}\cdot\boldsymbol{\beta})|\boldsymbol{k}_{\rm eff}||\boldsymbol{g}|T^2.\tag{4}$$

The residue phase shift which courses the systematic error induced by tilting is expressed as follows:

$$\Delta\Phi_{\rm tilt}=(-\alpha^2/2-\beta^2+\boldsymbol{\alpha}\cdot\boldsymbol{\beta})|\boldsymbol{k}_{\rm eff}||\boldsymbol{g}|T^2.\tag{5}$$

Since α and β are small, they can be expressed as $\boldsymbol{\alpha}=(\alpha_x,\alpha_y)$, and $\boldsymbol{\beta}=(\beta_x,\beta_y)$,[31] and the deviation of g-value can be expressed as

$$\frac{\delta g_{\rm tilt}}{g}=\alpha_x\beta_x+\alpha_y\beta_y-(\alpha_x^2+\alpha_y^2)/2-(\beta_x^2+\beta_y^2).\tag{6}$$

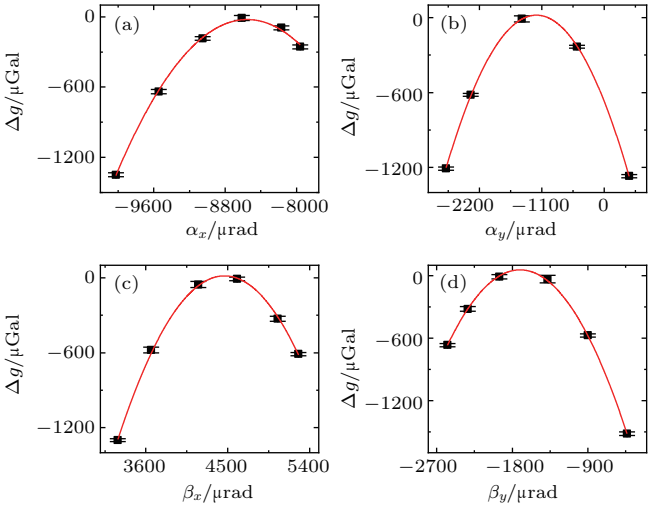


Fig. 2. The measured g-value varying the tilt angles in the third round adjustment. The black squares with error bars correspond to the experimental data, and the red curves are the parabolic fits. The extreme points are $\alpha_{x0}=-8553.4$ μrad, $\alpha_{y0}=-1193.3$ μrad, $\beta_{x0}=4459.0$ μrad, and $\beta_{y0}=-1706.0$ μrad.

As the four angles can be controlled by the four actuators independently, we can tune one while maintaining the other three fixed with monitoring the measured g value. For each round, we tune the four angles one by one in serial and record the measured g-value accordingly. Thus, we can get four sets of g-angle curves and make the parabolic fit to obtain the extreme point for each. When varying α_x and keep the other three fixed, equation (6) could be transformed to

$$\frac{\delta g_{\rm tilt}}{g}=-(\alpha_x-\beta_x)^2/2+C_1,\tag{7}$$

where C_1 is a constant. The extreme point of Eq. (7) is $\alpha_x=\beta_x$. In the following, when varying β_x, equation (6) turns to be

$$\frac{\delta g_{\rm tilt}}{g}=-(\beta_x-\alpha_x/2)^2+C_2,\tag{8}$$

where C_2 is another constant. The extreme point of Eq. (8) is $\beta_x=\alpha_x/2$. Similarly, for the varying of α_y and β_y, the extreme points are β_y and $\alpha_y/2$, respectively.

From the analysis we know that only the single adjustment round cannot correct the Raman beams along vertical direction precisely and cannot eliminate the tilting induced systematic error. After applying many adjustment rounds and setting the angles to the corresponding extreme points for each round, the four tilt angles decrease to a convergence value, as seen in Table 1. In this way, we can finally make $\boldsymbol{k}_{\rm eff}$ parallel with $\boldsymbol{g}$.

Table 1. The residues of the four tilt angles, which vary according to the adjustment rounds.

	Initial value	Round 1	Round 2	Round N
α_x	α_{x0}	β_{x0}	$\beta_{x0}/2$	$\beta_{x0}/2^{N-1}$
α_y	α_{y0}	β_{y0}	$\beta_{y0}/2$	$\beta_{y0}/2^{N-1}$
β_x	β_{x0}	$\beta_{x0}/2$	$\beta_{x0}/4$	$\beta_{x0}/2^N$
β_y	β_{y0}	$\beta_{y0}/2$	$\beta_{y0}/4$	$\beta_{y0}/2^N$

After the tilting angles are set to the extreme points at the end of each round, we start to perform the next adjustment round. The extreme points with varying adjustment rounds is shown in Fig. 3(a). We can see that in the first 6 adjustment rounds, the extreme points are monotonically approaching a convergence value, and fit with the theoretical results well. From round 6 to round 8, the extreme points keep unchanged with only small fluctuations. This indicates that the limits of the tilt-meter resolution are reached. The uncertainties (standard deviations) of the tilt angles after the adjustment are as follows:

$$\begin{aligned}\delta\alpha_x&=\pm37.2\ \mu\text{rad},\\ \delta\alpha_y&=\pm7.3\ \mu\text{rad},\\ \delta\beta_x&=\pm6.3\ \mu\text{rad},\\ \delta\beta_y&=\pm8.9\ \mu\text{rad}.\end{aligned}\tag{9}$$

Converting the uncertainty of the tilt angle to the uncertainty of the g value with Eq. (6), we obtained an uncertainty of g value due to the tilt of the Raman beams which is $\delta g_{\rm tilt}=(+0,-0.8)$ μGal.

We have measured g at the beginning of each adjustment round, as shown in Fig. 3(b). It is clear that the measured g-values are increasing with the adjustment round, which means that the real tilt of the Raman lasers becomes smaller and smaller. After 5 rounds, the g-value converges.

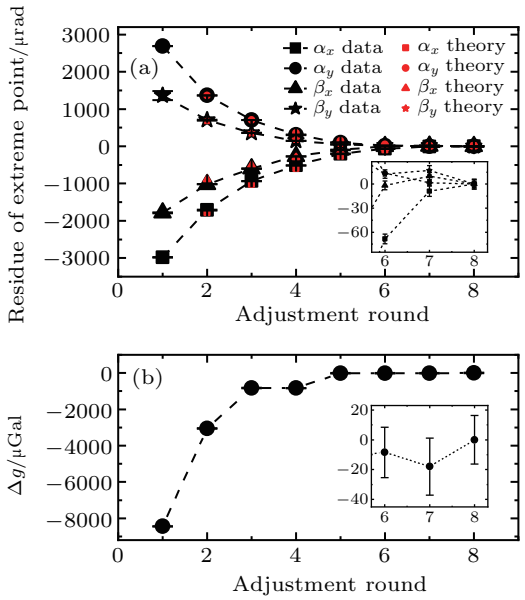


Fig. 3. (a) The residues of extreme points of the four tilt angles due to the adjustment rounds. The residues were obtained by subtracting the offset values (the extreme points of round 8) from the extreme points of each round. The black symbols and bars indicate the experimental data, and the red symbols indicate the theoretical values (see Table 1). The inset figure shows an enlarged view of the last three adjustment rounds. (b) The measured g-values due to the adjustment rounds. The g-values have been subtracted by the Earth tide and the g-value of round 8. The inset figure shows an enlarged view of the last three adjustment rounds.

3.1. Tilt drift and realtime measurement

During the continuous measurement of the gravity acceleration over long time, we have observed the drifts of the tilting angles due to the relaxing of the mechanical structure of the gravimeter, which also affects the measurement results. The drifts of the four tilting angles are continuously monitored by the tilt meters. Figure 4(a) presents the drifts of the tilting angles over 36 hours. We can find that α_x and α_y are quite stable but β_x and β_y have a nearly linear drift. The calculated drift of the g measurement is shown in Fig. 4(b). It has a nearly linear drift in the first 30 hours with the rate of 0.142 μGal/h.

The continuous measurement of g in our laboratory starts on December 12, 2018. We take the data for the first 36 hours, as shown in Fig. 5(a). By subtracting the measurement data with the calculated tide fluctuation with solid-tide model, the residue (Fig. 5(a) lower part) is obtained. The Allan deviation of the g measurement is shown in Fig. 5(b) (red curve). The sensitivity of our gravimeter is 5.5 μGal@300 s, correspond to about 94 μGal/$\sqrt{\text{Hz}}$. We subtract the calculated drift of g (Fig. 4(b)) from the measurement value to calculate the Allan deviations (Fig. 5(b) (blue curve)). The comparison (Table 2) shows that the stability of our atomic gravimeter is not affected much by the drifting of the tilting angle.

Table 2. Comparison between the performances without and with tilt compensation (TC).

TC	Stability (μGal@9560 s)	Stability (μGal@19121 s)	Stability (μGal@38241 s)
Without	3.97	5.18	3.82
With	3.94	4.96	2.97

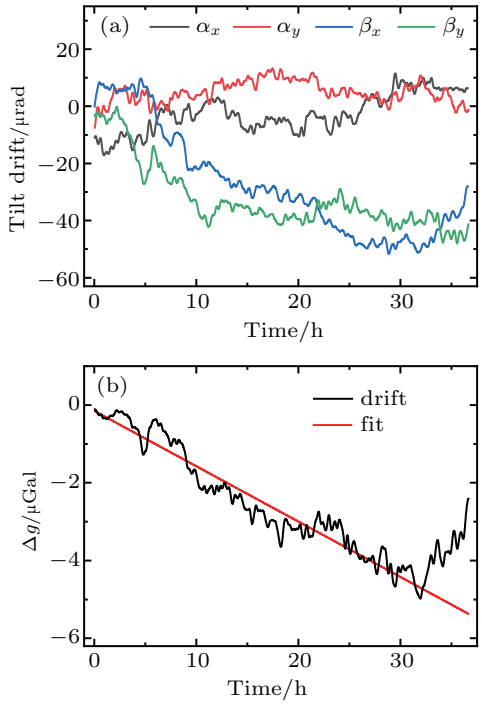


Fig. 4. Variations over time of the four tilt angles. (a) The observed drifts of four angles α_x, α_y, β_x and β_y. (b) The calculated drift of g-value corresponding to the drifts of the tilting angles.

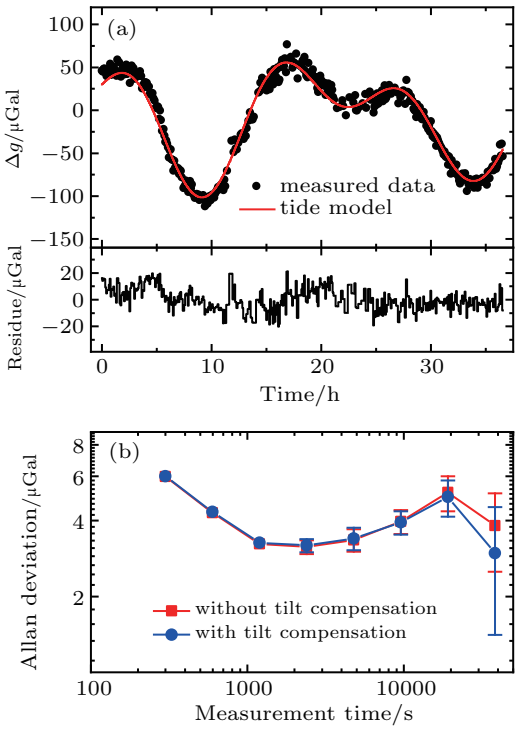


Fig. 5. Continuous g measurement on December 12, 2018. (a) The black points indicate the measured data of g, each datum is an average of g measurement over atom falling of 900 times (approximately 298 s). The red line is the calculation from the Earth tide model. The residue shows the difference between the measured g and the tide model. (b) Allan deviation of the g measurement with and without tilt drift correction.

4. Conclusion

We have found a practical approach to precisely adjust the Raman laser beams in an absolute atomic gravimeter. By applying the multi-stage adjustment, the measured g grad-

ually converges to an extreme maximum value, which tells us that the pointing of the Raman lasers is parallel to $\boldsymbol{g}$ direction. For our gravimeter USTC-AG02, the systematic error due to the tilting has been well eliminated and becomes $0\ (+0, -0.8)$ μGal considering the uncertainty. The long-term drift of the tilting angle has also been monitored and the compensation was applied during the continuous measurement of g. Our method is especially suitable for the compact and portable gravimeters used for the mobile gravity measurements and observations.

References

[1] de N, Darrigol O and Schlaudt O 2019 *The Reform of the International System of Units (SI)* (London: Routledge) p. 131

[2] Marson I and Faller J E 1986 *J. Phys. E: Sci. Instrum.* **19** 22

[3] Rice H, Kelmenson S and Mendelsohn L 2004 *Proceedings of the IEEE Position Location and Navigation Symposium*, April 26–29, 2004, Monterey, USA, pp. 618–624

[4] Prothero W A and Goodkind J M 1968 *Rev. Sci. Instrum.* **39** 1257

[5] Riccardi U, Rosat S and Hinderer J 2011 *Metrologia* **48** 28

[6] Okubo S, Yoshida S, Sato T, Tamura Y and Imanishi Y 1997 *Geophys. Res. Lett.* **24** 489

[7] Liard J and Gagnon C 2002 *Metrologia* **39** 477

[8] Li C J, Xu J Y, Feng J Y, Su D W and Wu S Q 2015 *Proc. Volume 9446 Ninth International Symposium on Precision Engineering Measurement and Instrumentation*, March 6, 2015, Changsha, China

[9] Kasevich M and Chu S 1991 *Phys. Rev. Lett.* **67** 181

[10] Peters A, Chung K Y and Chu S 1999 *Nature* **400** 849

[11] Peters A, Chung K Y and Chu S 2001 *Metrologia* **38** 25

[12] Gouet J L, Mehlstaubler T, Kim J, Merlet S, Clairon A, Landragin A and Santos F P D 2008 *Appl. Phys. B* **92** 133

[13] Zhou L, Xiong Z Y, Yang W, Tang B, Peng W C, Wang Y B, Xu P, Wang J and Zhan M S 2019 *Chin. Phys. B* **28** 013701

[14] Wang J 2015 *Chin. Phys. B* **24** 053702

[15] Wang Q Y, Wang Z Y, Fu Z J and Lin Q 2016 *Chin. Phys. B* **25** 123701

[16] Abend S, Gebbe M, Gersemann M, Ahlers H, Muntinga H, Giese E, Gaaloul N, Schubert C, Lammerzahl C, Ertmer W, Schleich W P and Rasel E M 2016 *Phys. Rev. Lett.* **117** 203003

[17] Cheng Y, Tan Y J, Zhou M K, Duan X C, Shao C G, Hu Z K 2018 *Chin. Phys. B* **27** 030303

[18] Huang P W, Tang B, Chen X, Zhong J Q, Xiong Z Y, Zhou L, Wang J and Zhan M S 2019 *Metrologia* **56** 045012

[19] Wu X, Pagel Z, Malek B S, Nguyen T H, Zi F, Scheirer D S and Muller H 2019 *Sci. Adv.* **5** eaax0800

[20] Wang S K, Zhao Y, Zhuang W, Li T C, Wu S Q, Feng J Y and Li C J 2018 *Metrologia* **55** 360

[21] Hu Z K, Sun B L, Duan X C, Zhou M K, Chen L L, Zhan S, Zhang Q Z and Luo J 2013 *Phys. Rev. A* **88** 043610

[22] Freier C, Hauth M, Schkolnik V, Leykauf B, Schilling M, Wziontek H, Scherneck H G, Muller J and Peters A 2016 *J. Phys.: Conf. Ser.* **723** 012050

[23] Wu S, Feng J, Li C, Su D, Wang Q, Hu R, Hu L, Xu J, Ji W, Ullrich C *et al.* 2020 *Metrologia* **57** 07002

[24] Altin P A, Johnsson M T, Negnevitsky V, Dennis G R, Anderson R P, Debs J E, Szigeti S S, Hardman K S, Bennetts S, Mcdonald G D, Turner L D, Close J D and Robins N P 2013 *New J. Phys.* **15** 023009

[25] Senger A *A mobile atom interferometer for high-precision measurements of local gravity* (PhD Dissertation) (Berlin: Humboldt University), pp. 54–55

[26] Hauth M, Freier C, Schkolnik V, Senger A, Schmidt M and Peters A 2013 *Appl. Phys. B* **113** 49

[27] Menoret V, Vermeulen P, Moigne N L, Bonvalot S, Bouyer P, Landragin A and Desruelle B 2018 *Sci. Rep.* **8** 12300

[28] Zhou M K, Luo Q, Chen L L, Duan X C and Hu Z K 2016 *Phys. Rev. A* **93** 043610

[29] Trimeche A, Langlois M, Merlet S and Santos F P D 2017 *Phys. Rev. Appl.* **7** 034016

[30] Louchet-Chauvet A, Farah T, Bodart Q, Clairon A, Landragin A, Merlet S and Santos F P D 2011 *New J. Phys.* **13** 065025

[31] Wu B, Cheng B, Fu Z J, Zhu D, Zhou Y, Weng K X, Wang X L and Lin Q 2018 *Acta. Phys. Sin.* **67** 190302 (in Chinese)